Ordering process of colloidal crystal in semidilute aqueous suspensions

Tsuyoshi Yoshiyama
Department of Physics, Faculty of Science, Kyoto Sangyo University, Kyoto 603, Japan
(Received 3 September 1985; revised 7 October 1985)

The time-dependent ordering processes of colloidal crystals in polystyrene latex suspensions were investigated by an optical diffraction method for specimens of concentration 4.0–10 vol%. He–Ne and Ar laser beams were used to produce a point light source with strong intensity in the suspensions, and Kossel lines caused by crystal diffraction of a divergent laser beam from the point source were analysed to examine the crystal structure and to determine the lattice constants. The results showed that the crystal was formed by way of intermediate ordering processes as follows: liquid state→two-dimensional hcp structure→random layer structure→structure with one sliding degree of freedom→stacking disorder structure→FCC with (111) twin→normal FCC structure.

(Keywords: colloidal crystal; ordering; Kossel line; polystyrene latex; structure change)

INTRODUCTION

A colloidal crystal is formed in monodisperse charged polystyrene latex suspensions. Since interparticle distances in the colloidal crystal are of the order of visible light wavelengths, particles constituting the crystal can be directly observed with an optical microscope[1,2]. By this means it is possible not only to examine a crystal structure and interparticle distances but also to observe the surface state of the crystal, crystal defects and the aspect of the crystal growth. However it is very difficult to analyse quantitatively the detailed crystal structure and the accurate lattice constants because the observations are limited to two dimensions and the resolving power is low.

The facts discovered by direct optical observations (e.g. interparticle distance $>1\,\mu m$ in the colloidal crystal in the case of dilute suspensions and a problem with respect to the stability of the crystal to additional impurity salts) cannot be interpreted by DLVO theory so that new ideas are required about interparticle interactions in this system[3].

Optical diffraction[4–6] is a powerful method for studying crystal structure, lattice constants, interparticle distances and the stability of the crystal to the amount and the kind of impurities. Kossel line analysis[7], which involves optical diffraction, is a particularly apt method for studying colloidal crystal structure because information with respect to some reciprocal lattice vectors is gained in the static state of the specimen while in the normal diffraction method it is necessary to move the specimen (by oscillation or rotation) in order to obtain diffraction spots when a monochromatic beam is used. A fine laser beam directed through an incident pinhole aperture produces a high intensity point light source in the disordered region of the colloidal crystal. Parts of the divergent beams from the point light source that satisfy the diffraction condition for the surrounding crystal planes are reflected to produce Kossel lines, which give highly accurate interparticle distances between the latex particles constituting the colloidal crystal, crystal orientations and crystal structure. From the analyses of the Kossel lines it has been precisely shown in a previous paper[8] how interparticle distances in the colloidal crystals vary depending on particle concentration (0.6–9.8 vol%). It was also reported that the structure of the polystyrene colloidal crystal is BCC for dilute specimens with volume fraction $\phi < 1.5$ vol% and FCC for concentrated specimens ($\phi \geq 4.0$ vol%) and that for intermediate concentrations (1.5 vol% $\leq \phi < 4.0$ vol%) there is a change of structure from FCC to BCC at an early stage of ordering.

In this paper the time-dependent structural development of colloidal crystals in concentrated latex suspensions ($\phi \geq 4.0$ vol%) is elucidated by Kossel line analysis. No Kossel lines have been observed at the initial stage of ordering but the structure development could begin with the formation of two-dimensional hexagonal close packed layers, an inference drawn from the experimental results of the optical diffraction done by Clark *et al.*[6] The results of Kossel line analyses show that formation of a random layer structure, in which the interlayer distance is definite but the lateral phase shift between adjacent layers is perfectly random, succeeds the two-dimensional hexagonal close packed structure. Two degrees of freedom of displacement in a layer at this stage are gradually frozen into one sliding degree of freedom. As the next stage there appears a stacking disorder structure, which is composed of a layer sequence in which each layer occupies one possible site of two-fold choice with statistically determined ratio on stacking closest packed layers. As ordering progresses further, a face centred cubic structure with (111) twin plane is produced from the stacking disorder structure and, finally, the structure of the colloidal crystal in the concentrated latex suspensions reaches a normal face centred cubic structure.

EXPERIMENTAL

Suspensions of sulphonate-modified polystyrene latices were deionized by ultrafiltration until the electric

0032-3861/86/060827-07$03.00

conductivity reached a minimum value ($\leqslant 1.5$ μmho). Each latex particle had a mean diameter $\bar{D} = 1560$ Å and a surface charge -3×10^4 e. The specimens of concentration in the range 4.0–10 vol%, were poured into a clean rectangular quartz cuvette (length 40 mm, width 10 mm and thickness 1 mm) after deionizing by anion and cation exchange resins. The cuvette was fixed on a goniometer head. The specimens were examined by laser (He–Ne: $\lambda_{air} = 6328$ Å and Ar: $\lambda_{air} = 4880$ Å) beam diffraction method using a cylindrical camera ($2R = 57.3$ mm) in a dark room at room temperature. The backward scattering beams were photographed (Fuji FG film) to overcome the lower transparency to the beam at high concentration and to obtain highly accurate measurements, most of which were made with the incident beam normal to the wide surface plane of the cuvette. A fine laser beam directed through an incident aperture with a 1.0 mm^2 pinhole randomly interacts with a disordered region that exists between crystal grains in the suspension so that the region becomes a point light source of divergent beams. Some directions of the backward scattered light satisfy the diffraction condition for lattice planes of surrounding crystallites, so that the directions of the beams are deflected by the crystallites and depleted lines (Kossel lines) are produced in backward divergent beams. The directions that satisfy the diffraction condition for a crystal lattice plane form a cone (Kossel cone) whose central axis is parallel to a reciprocal lattice vector representing the crystal lattice plane[9]. The semivertical angle of the cone determines a magnitude of the reciprocal lattice vector (a reciprocal of the interplanar distance). Therefore the Kossel cones appearing in backward diffraction enable determination of the crystal structure and lattice constants of the colloidal crystals.

Since photographed Kossel lines were deformed owing to the use of a cylindrical camera and by the effects of refraction at suspension-quartz and quartz-air interfaces, data correction was necessary before the analyses. Correcting the deformation due to the use of a cylindrical camera was simple because the diameter of the camera was determined with high accuracy. Refraction was corrected by Snell's law using the refractive indices of $n_s = 1.33 + 0.27\,C$ (where C is concentration)[4] for the specimens, $n_{air} = 1.00$, and n_q(He–Ne) = 1.54 and n_q(Ar) = 1.55 for the quartz plate, although the refractive effect of the quartz plate was only a parallel displacement of beam of less than 0.7 mm (the thickness of quartz plate of the cuvette).

In principle, measurement of the coordinates of three points on a curve forming a Kossel cone determine the direction of the central axis and the semivertical angle of the cone. However, small measurement errors lead to large discrepancies in results for a curve with small curvature. In such a case the minimum angle θ_{min} among angles which the incident beam direction forms with the generating lines of the Kossel cone was measured. If the indices of the Kossel cones were assumed in the light of the symmetry of the disposition of the Kossel cones, it was possible to determine the angles θ_0 between the incident beam direction and the central axes of Kossel cones (the direction of the reciprocal lattice vectors). The interplanar spacing was determined from the difference $\theta_0 - \theta_{min}$. This procedure was repeated until the consistency in the directions and magnitudes of reciprocal lattice vectors was obtained for all Kossel lines in a photograph.

Since the angles between all possible reciprocal lattice vectors in the cubic system are fixed by symmetry, it is possible to predict the range of the lattice constant for the cubic crystals from the relative dispositions of Kossel cones without precise analysis. As a pre-analysis of Kossel cones the lattice constants at which two Kossel cones with low indices contact each other was calculated (*Table 1*).

The argon laser beam was mainly used for high concentration specimens because the limiting sphere of radius $2/\lambda$ ($\lambda = \lambda_{air}/n_s$) contains a larger portion of reciprocal space the shorter the wavelength.

RESULTS

All specimens immediately after placing the suspensions of polystyrene latices in the quartz cuvettes gave no diffraction effects. When the ordering began in the suspensions broad diffraction spots were first observed. As ordering advanced, Kossel cones caused by the polystyrene colloidal crystals appeared on examination by optical diffraction by means of Ar or He–Ne laser beam.

In the first stage of the three-dimensional crystal formation only a Kossel cone that belonged to a reciprocal lattice vector parallel to the incident direction of a beam was observed. This Kossel cone developed to a 111 cone of FCC structure in the later stage of crystallization. No other Kossel cones appeared in spite of a larger lattice constant for contact with other 111 cones ($1\bar{1}\bar{1}$, $1\bar{1}1$, $\bar{1}11$ cones) if the crystal structure was face centred cubic (see *Table 1*). The aspect of this situation is shown in *Figure 1(a)*. The reciprocal lattice of the specimen in this stage is shown in *Figure 1(b)*.

In the second stage of crystal formation two Kossel lines in addition to a Kossel ring developing to a 111 ring were observed; this is shown in *Figure 2(a)*. The Kossel pattern in *Figure 2(a)* can be interpreted by a reciprocal lattice shown in *Figure 2(b)*.

With the development of ordering new Kossel cones appeared (*Figure 3(a)*). The reciprocal lattice is shown in *Figure 3(b)*. Six Kossel cones at 60° intervals crossed over the 111 Kossel ring.

FCC with 111 twin and normal FCC structure were observed at the final stage of order formation for specimens investigated (*Figures 4* and *5*). The only twin plane observed has been (111) in spite of crystallographic equality to {111} planes. The crystal plane parallel to the wide surface of the cuvette was a (111) plane although the

Table 1 Lattice constants (Å) at which a Kossel cone comes in contact with low indices Kossel cones

	He–Ne laser				Ar laser			
	111	$1\bar{1}1$	200	220	111	$1\bar{1}1$	200	220
111	(4120)	5047	5047	—	(3178)	3892	3892	—
$1\bar{1}\bar{1}$	5047	7137	5047	—	3892	5504	3892	—
$1\bar{1}1$	5047	(4120)	5047	7890	3892	(3178)	3892	6085
$\bar{1}11$	5047	7137	9663	7890	3892	5504	7452	6085
200	5047	5047	(4758)	6729	3892	3892	(3669)	5189
020	5047	9663	6729	6729	3892	7452	5189	5189
002	5047	5047	6729	8241	3892	3892	5189	6355
220	—	—	6729	(6729)	—	—	5189	(5189)
022	—	7890	8241	7770	—	6085	6355	5992
202	—	—	6729	7770	—	—	5189	5992

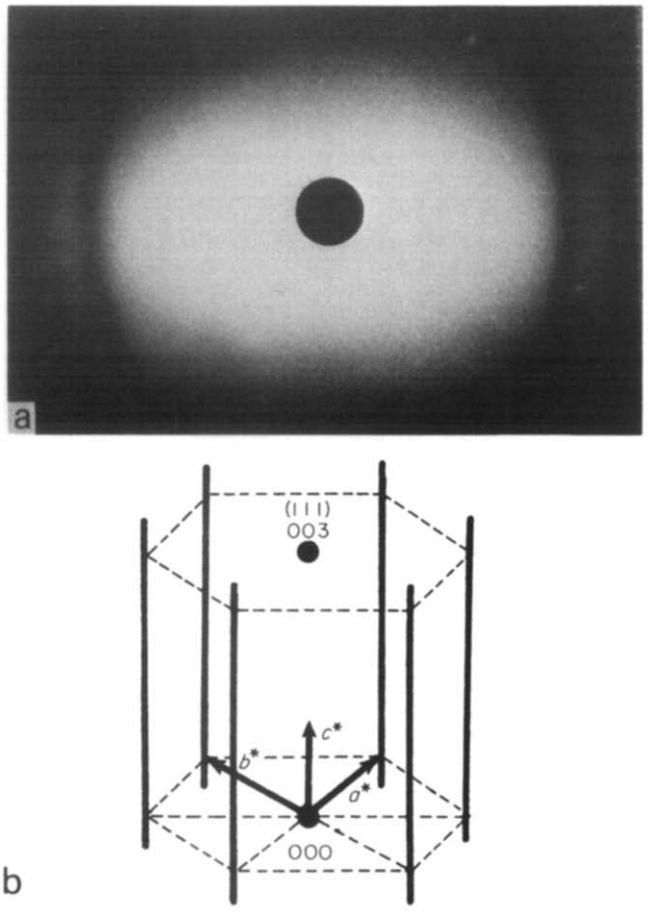

Figure 1 (a) A Kossel ring observed in a specimen of 8.0 vol% polystyrene latex suspension with Ar laser beam. The interplanar distance d corresponding to this Kossel ring is 2335 Å, so that the lattice constant $a_0 = 3^{\frac{1}{2}}d = 4044$ Å is larger than the value at which $11\bar{1}$, 200 etc. come into contact with the 111 Kossel cone; (b) in this reciprocal lattice only the 003 (111 in FCC) reciprocal lattice vector gives a distinct Kossel ring because the Kossel lines originated in reciprocal rods continuously extended over an angle range

rotation of the crystal about the [111] axis was free. As the beam was incident perpendicular to the wide plane of the cuvette, the incident direction of the beam was [111]. In *Figure 6* the reciprocal lattices of normal FCC structure and FCC with (111) twin are shown. *Table 2* shows the angles between two reciprocal lattice vectors and the interplanar spacings evaluated by analysis of the Kossel cones in *Figure 5*. The calculated angles from the reciprocal lattice shown in *Figure 6* are given in parentheses. The correspondence between experimental and calculated values is satisfactory for all reciprocal lattice vectors.

DISCUSSION

In an early stage of three-dimensional order formation a single Kossel ring belonging to a reciprocal lattice vector parallel to the incident beam direction, normal to the cuvette surface, has observed for all specimens examined in this experiment. So, the Kossel ring originates in the parallel plane stacking to the surface plane of the cuvette. The Kossel ring can be indexed as 111 of FCC from the result of the following ordering process although it is impossible to determine the crystal structure from a single Kossel ring. If the structure is face centred cubic, however, $11\bar{1}$, $1\bar{1}1$, $11\bar{1}$, 200, 020 and 002 Kossel lines must intersect the 111 Kossel ring because a lattice constant $a_0 = 4404$ Å estimated from the 111 Kossel ring is larger than their contact condition $a_0 = 3892$ Å. The lack of these Kossel lines suggests that the crystal structure in an early stage of order formation would be a kind of modified FCC structure. Warren[10] and Franklin[11] showed a 'random layer structure' as a structure of amorphous graphite. In this structure two-dimensional close packed planes are stacked at a definite planar distance but the relative phase between the planes is perfectly random. The reciprocal lattice of this structure is shown in *Figure 1(b)*. In this structure the 003 (111 in FCC) reciprocal lattice vector gives a distinct Kossel ring but $hk\beta$ reciprocal rods give diffuse halos indistinguishable from the background intensity.

During the progress of order formation new Kossel lines appear in addition to the 111 Kossel ring. The two lines cut across the 111 Kossel ring as shown in *Figure 2(a)*. The reciprocal lattice corresponding to this stage is shown in *Figure 2(b)* and a pair of reciprocal rods in *Figure 1(b)* turns into a pair of reciprocal lattice points. In real space it can be interpreted by a model that two dimensional close packed layers freely slip along one direction (e.g. $[1\bar{1}0]$ in FCC) in the layer although interplanar distance d_{111} is definite. A similar model was proposed by Clark and Ackerson[6] although the packing of layers of their model was the same as that of body-

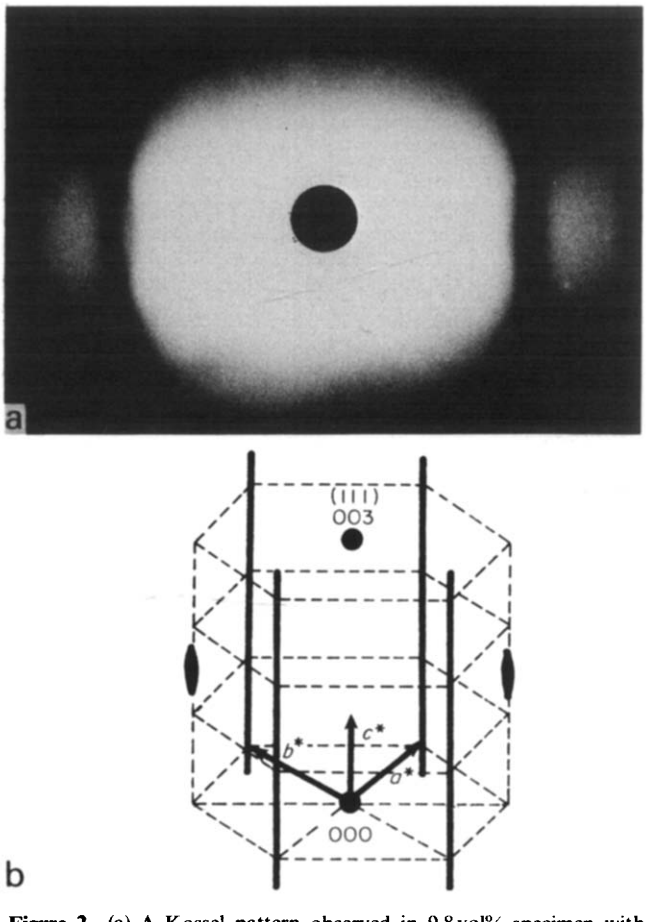

Figure 2 (a) A Kossel pattern observed in 9.8 vol% specimen with Ar laser beam. The lattice constant $a_0 (= 3^{\frac{1}{2}}d_{111})$ estimated from the analysis of the 111 Kossel ring is 3984 Å and the value is nearly equal to a lattice constant (3982 Å) at which 200 Kossel cone comes into contact with the 111 Kossel cone; (b) only a pair of reciprocal rods in *Figure 1(b)* is concentrated into a pair of points in reciprocal lattice so that two reciprocal lattice vectors give distinct Kossel lines

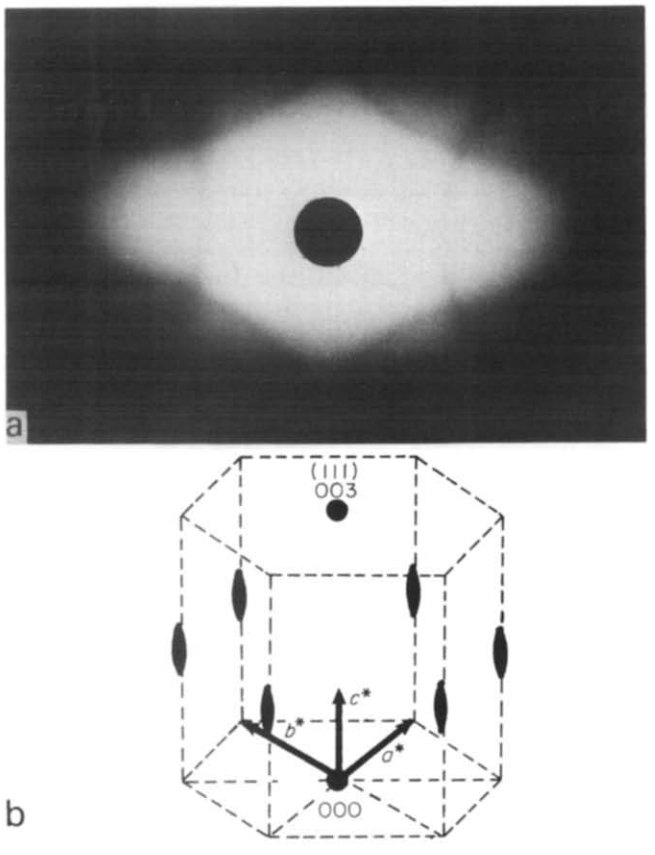

Figure 3 (a) Kossel pattern observed at the third stage of order formation in 3.5 vol% specimen with He–Ne laser. The lattice constant, $a_0 = 5564 \pm 50$ Å, can be estimated from the 111 ring and other Kossel lines; (b) during the development of order formation all reciprocal rods (*Figure 1(b)*) are concentrated into points. The reciprocal lattice shown is at $\alpha = 0.5$, and six equivalent Kossel lines crossing with the 111 Kossel ring can be observed at this situation

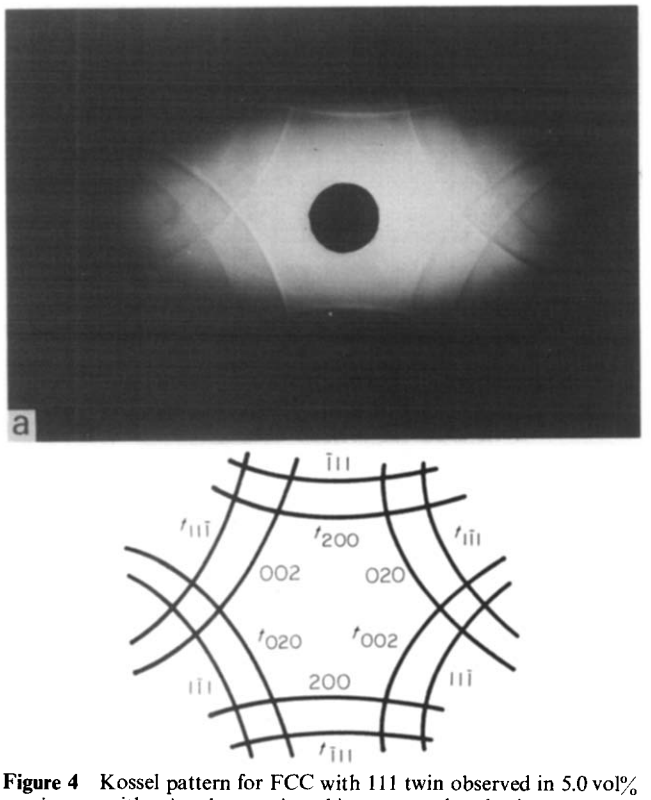

Figure 4 Kossel pattern for FCC with 111 twin observed in 5.0 vol% specimen with Ar laser. At this stage the lattice constant $a_0 = 4697 \pm 51$ Å. Indices of Kossel cones in the photo are shown below. The 111 Kossel ring cannot be observed because the semivertical angle of the cone becomes too large for backward scattering

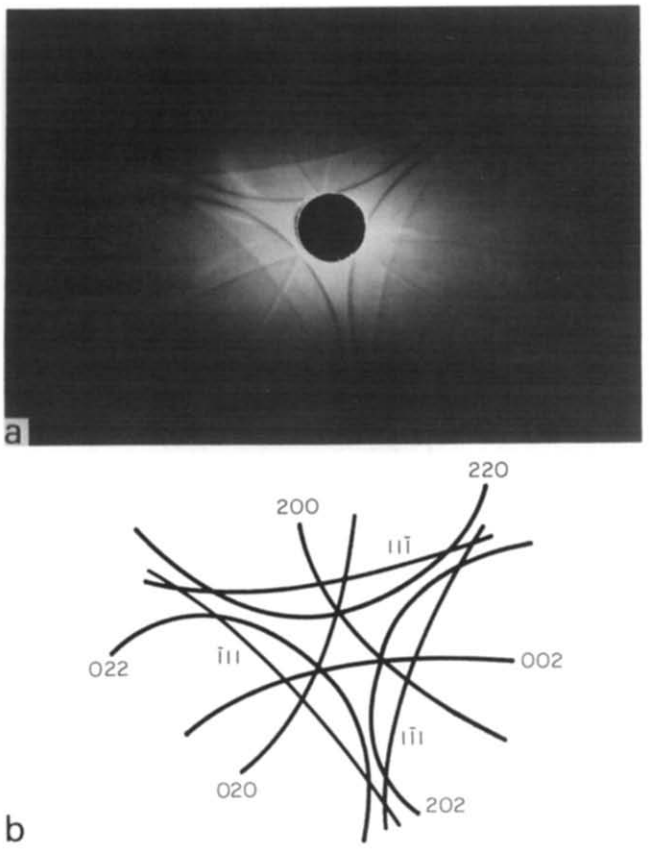

Figure 5 Kossel pattern for normal FCC structure with He–Ne laser. Indices of Kossel lines are shown below

centred cubic. In such a model the reciprocal lattice points are shifted along c^* direction by the stacking disorder from normal positions of FCC reciprocal lattice points. Nevertheless two new Kossel lines representing the shifted reciprocal lattice vectors come into contact with the 111 Kossel ring at the same time. This is proved in Appendix A. The shift value x can be experimentally determined for each pair of cones (see Appendix B) so that the lattice constant $a_0 (= \sqrt{3} d_{111})$ can be estimated from the 111 Kossel ring and other line pairs. The value of x and the lattice constant are shown in *Table 3*.

In the next step six new Kossel lines appear in addition to the 111 ring. This case is shown in *Figure 3(a)*. In the reciprocal lattice shown in *Figure 3(b)* six reciprocal rods in *Figure 1(b)* are turned together into six reciprocal lattice points. A structure in real space corresponding to this reciprocal lattice is a 'stacking disorder structure', which is composed of stacking of statistically distributed two-dimensional hexagonal close-packed layers. Wilson[12], Paterson[13] and Kakinoki[14] analysed the diffuse scattering intensity distributions depending on the probability, α, of the hexagonal layer sequence. The relation between the probability, α, and the shift value, x, of the reciprocal lattice point is $\alpha = 3x$.

At a final stage of ordering FCC twin structure and normal FCC structure are formed. The aspects of these structures are shown in *Figures 4* and *5* with the indices of the Kossel cones. From the ordering sequence described above it is supposed that the twin plane is limited to the (111) plane. Although BCC structure has been observed in dilute specimens, it seems that FCC structure is a thermodynamically stable structure for high concentration specimens.

The order formation sequence in polystyrene latex suspension with concentration >4.0 vol% is as follows: liquid state→two-dimensional hcp structure→random layer structure→structure with one slipping degree of freedom→stacking disorder structure→FCC with (111) twin→normal FCC structure.

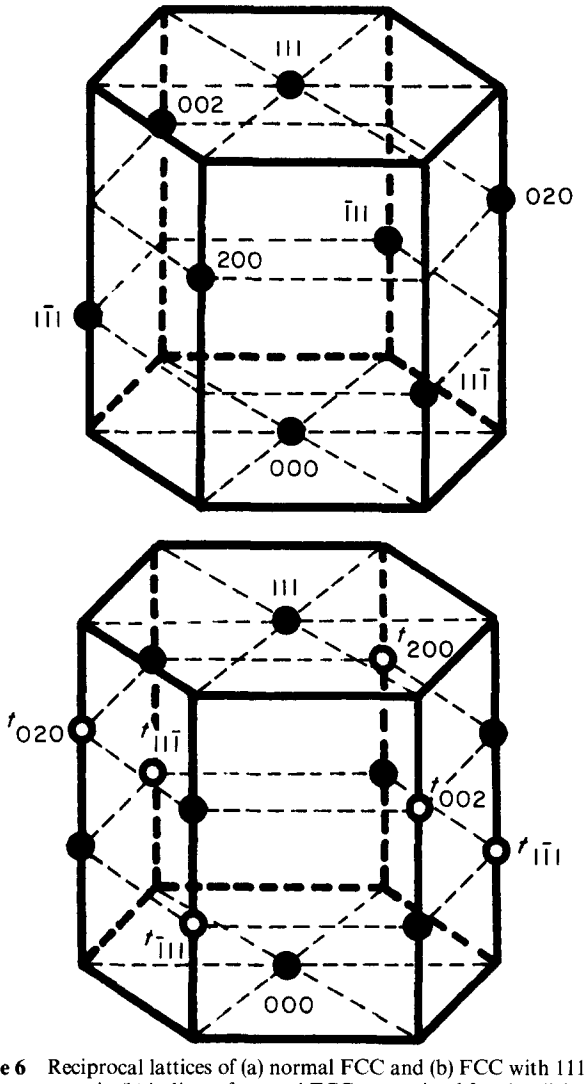

Figure 6 Reciprocal lattices of (a) normal FCC and (b) FCC with 111 twin structures; in (b) indices of normal FCC are omitted for simplicity

In suspensions with low concentration (<3.5 vol%) the structure of the colloidal crystal is developed to BCC structure in the final stage, and the structure change is as follows: normal FCC structure→BCC with $(12\bar{1})$ twin→normal BCC structure. The detailed mechanism of this structural change will be presented elsewhere.

ACKNOWLEDGEMENT

The author thanks Prof. N. Ise for kindly supplying the suspension specimen and Prof. K. Asai and Prof. I. Sogami for their helpful discussions and encouragement of this work.

APPENDIX A

$$g'_{\bar{1}11} = g_{\bar{1}11} + xg_{111} \quad \text{(A1)}$$

$$g'_{200} = g_{200} - xg_{111} \quad \text{(A2)}$$

and

$$|g_{111}| = |g_{\bar{1}11}| = \sqrt{3}a^* \quad \text{(A3)}$$

$$|g_{200}| = 2a^* \quad \text{(A4)}$$

where a^* is the magnitude of basal vector $\boldsymbol{a}^*$ in the reciprocal lattice of face centred cubic and x is a shift value

Table 3 Lattice constant a_0 and the values of α, the probability of layer sequence A–C, and x, the shift values of the reciprocal lattice points from the normal position in FCC structure, determined from experimental data (*Figures 2(a), 3(a)*)

x	α	a_0 (Å)		
0.16_3	0.49	3896	pair	*Figure 2(a)*
		3898	111	
0.16_7	0.50	5594	b–b′	*Figure 3(a)*
0.14_4	0.43	5637	c–c′	
0.14_8	0.45	5607	d–d′	
		5564	111	

Table 2 FCC crystal orientation correspondence and interplanar distances d_{hkl}

	202	022	220	002	020	200	$1\bar{1}1$	$\bar{1}11$	$11\bar{1}$
202	0.0	58.6	60.6	44.4	90.0	44.1	35.3	89.3	90.0
	(0.0)	(60.0)	(60.0)	(45.0)	(90.0)	(45.0)	(35.3)	(90.0)	(90.0)
022	58.6	0.0	60.8	43.6	46.6	89.9	88.7	35.3	92.0
	(60.0)	(0.0)	(60.0)	(45.0)	(45.0)	(90.0)	(90.0)	(35.3)	(90.0)
220	60.6	60.8	0.0	90.0	44.8	46.9	90.1	89.9	35.3
	(60.0)	(60.0)	(0.0)	(90.0)	(45.0)	(45.0)	(90.0)	(90.0)	(35.3)
002	44.4	43.6	90.0	0.0	90.2	88.1	54.6	54.8	125.2
	(45.0)	(45.0)	(90.0)	(0.0)	(90.0)	(90.0)	(54.7)	(54.7)	(125.3)
020	90.0	46.6	44.8	90.2	0.0	91.6	125.3	54.9	55.9
	(90.0)	(45.0)	(45.0)	(90.0)	(0.0)	(90.0)	(125.3)	(54.7)	(54.7)
200	44.1	89.9	46.9	88.1	91.6	0.0	52.2	125.2	56.0
	(45.0)	(90.0)	(45.0)	(90.0)	(90.0)	(0.0)	(54.7)	(125.3)	(54.7)
$1\bar{1}1$	35.3	88.7	90.1	54.6	125.3	52.2	0.0	109.4	108.2
	(35.3)	(90.0)	(90.0)	(54.7)	(125.3)	(54.7)	(0.0)	(109.5)	(109.5)
$\bar{1}11$	89.3	35.3	89.9	54.8	54.9	125.2	109.4	0.0	110.8
	(90.0)	(35.3)	(90.0)	(54.7)	(54.7)	(125.3)	(109.5)	(0.0)	(109.5)
$11\bar{1}$	90.0	92.0	35.3	125.2	55.9	56.0	108.2	110.8	0.0
	(90.0)	(90.0)	(35.3)	(125.3)	(54.7)	(54.7)	(109.5)	(109.5)	(0.0)
d_{hkl}	2101	2107	2122	2973	2939	2922	3514	3514	3518
a_0					5968 ± 125				

along [111] from $\bar{1}11$, 200 etc. reciprocal lattice points.

$$g_{111}g_{\bar{1}11}=(\sqrt{3}a^*)^2/3=a^{*2} \tag{A5}$$

$$g_{111}g_{200}=(\sqrt{3}a^*)(2a^*)/\sqrt{3}=2a^{*2} \tag{A6}$$

$$g_{111}g'_{\bar{1}11}=g_{111}(g_{\bar{1}11}+xg_{111})=(1+3x)a^{*2} \tag{A7}$$

$$g_{111}g'_{200}=g_{111}(g_{200}-xg_{111})=(2-3x)a^{*2} \tag{A8}$$

$$\begin{aligned} g'^2_{\bar{1}11}&=g^2_{\bar{1}11}+2xg_{\bar{1}11}g_{111}+x^2g^2_{111}\\ &=(3+2x+3x^2)a^{*2} \end{aligned} \tag{A9}$$

$$\begin{aligned} g'^2_{200}&=g^2_{200}-2xg_{200}g_{111}+x^2g^2_{111}\\ &=(4-4x+3x^2)a^{*2} \end{aligned} \tag{A10}$$

When a 111′ Kossel cone comes into contact with a 111 Kossel cone,

$$g_{111}/\cos\theta_1=g'_{\bar{1}11}/\cos\theta_2 \tag{A11}$$

(see *Figure 7(a)*). Thus,

$$\begin{aligned} g_{111}g'_{\bar{1}11}&=(1+3x)a^{*2}\\ &=g_{111}g'_{\bar{1}11}\cos(\theta_1+\theta_2)\\ &=g'_{\bar{1}11}\{g'_{\bar{1}11}\cos^2\theta_1\\ &\quad-\sin\theta_1\sqrt{g^2_{111}-g'^2_{\bar{1}11}\cos^2\theta_1}\}\\ &=a^{*2}\sqrt{3+2x+3x^2}\{\sqrt{3+2x+3x^2}\cos^2\theta_1\\ &\quad-\sin\theta_1\sqrt{3-(3+2x+3x^2)\cos^2\theta_1}\} \end{aligned} \tag{A12}$$

$$\cos^2\theta_1=8/(3+2x+3x^2)(4-4x+3x^2) \tag{A13}$$

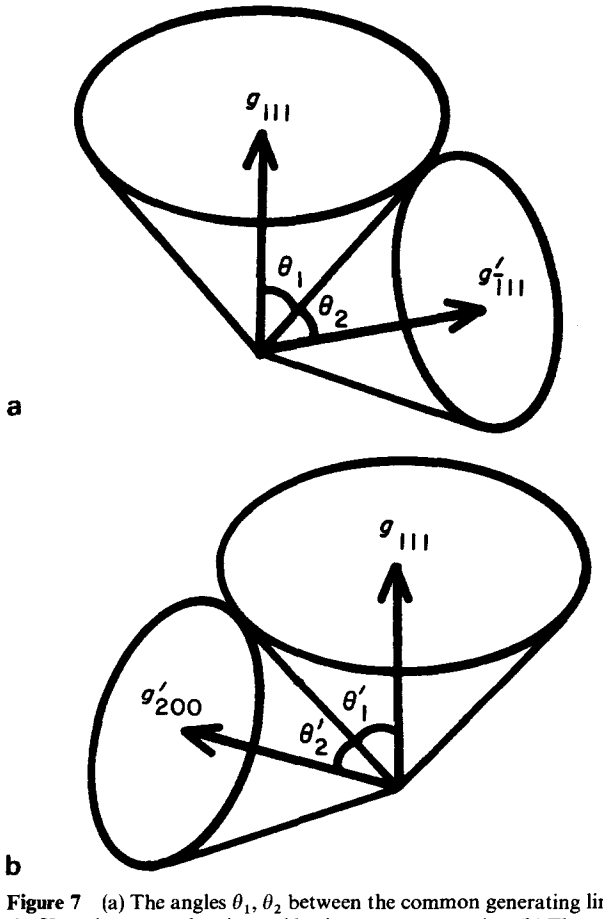

Figure 7 (a) The angles θ_1, θ_2 between the common generating line of the Kossel cones and reciprocal lattice vectors g_{111}, $g'_{\bar{1}11}$. (b) The angles θ'_1, θ'_2 between the common generating line of the Kossel cones and reciprocal lattice vectors g_{111}, g'_{200}

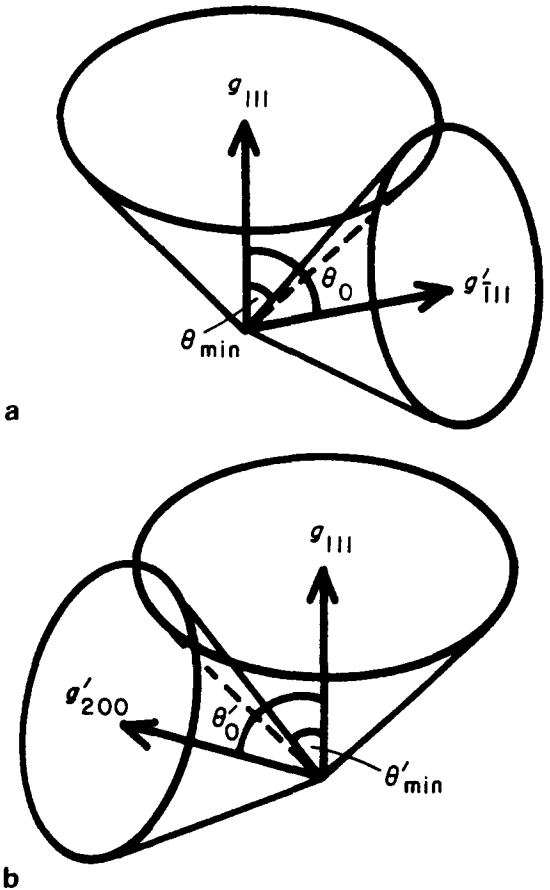

Figure 8 (a) The relative angle disposition of θ_0 and θ_{min}; (b) the relative angle disposition of θ'_0 and θ'_{min}

On the other hand,

$$g_{111}/\cos\theta'_1=g'_{200}/\cos\theta'_2 \tag{A14}$$

when a 200′ Kossel cone comes into contact with 111 Kossel cone (see *Figure 7(b)*)

$$\begin{aligned} g_{111}g'_{200}&=(2-3x)a^{*2}\\ &=g_{111}g'_{200}\cos(\theta'_1+\theta'_2)=g'_{200}\{g'_{200}\cos^2\theta'_1\\ &\quad-\sin\theta_1\sqrt{g^2_{111}-g'^2_{200}\cos^2\theta'_1}\}\\ &=a^{*2}\sqrt{4-4x+3x^2}\{\sqrt{4-4x+3x^2}\cos^2\theta'_1\\ &\quad-\sin\theta'_1\sqrt{3-(4-4x+3x^2)\cos^2\theta'_1}\} \end{aligned} \tag{A15}$$

$$\cos^2\theta'_1=8/(3+2x+3x^2)(4-4x+3x^2) \tag{A16}$$

Therefore $\theta_1=\theta'_1$ for any x value, that is, $\bar{1}11'$ and 200′ Kossel rings come into contact with 111 Kossel ring at the same time for any x value.

APPENDIX B

As shown in *Figure 8(a)*

$$\begin{aligned} g_{111}g_{\bar{1}11}&=g_{111}g'_{\bar{1}11}\cos\theta_0=\sqrt{3}a^*\sqrt{3+2x+3x^2}a^*\cos\theta_0\\ &=(1+3x)a^{*2} \end{aligned} \tag{B1}$$

$$\begin{aligned} \cos\theta_0&=(1+3x)/\sqrt{3(3+2x+3x^2)}\\ \sin\theta_0&=\sqrt{8}/\sqrt{3(3+2x+3x^2)} \end{aligned} \tag{B2}$$

$$g'_{\bar{1}11} = \frac{2}{\lambda}\cos(\theta_0 - \theta_{min})$$

$$= \frac{2/\lambda}{\sqrt{3(3+2x+3x^2)}}\{(1+3x)\cos\theta_{min} + \sqrt{8}\sin\theta_{min}\} \quad (B3)$$

$$= \sqrt{3+2x+3x^2}\,a^* \quad (B4)$$

$$(3+2x+3x^2)\frac{a^*\lambda}{2}\sqrt{3} = (1+3x)\cos\theta_{min} + 8\sin\theta_{min} \quad (B5)$$

On the other hand,

$$g_{111}g'_{200} = g_{111}g'_{200}\cos\theta'_0$$

$$= \sqrt{3}a^*\sqrt{4-4x+3x^2}\,a^*\cos\theta'_0$$

$$= (2-3x)a^{*2} \quad (B6)$$

$$\cos\theta'_0 = (2-3x)/\sqrt{3(4-4x+3x^2)}$$

$$\sin\theta'_0 = \sqrt{8}/\sqrt{3(4-4x+3x^2)} \quad (B7)$$

As shown in *Figure 8(b)*,

$$g'_{200} = \frac{2}{\lambda}\cos(\theta'_0 - \theta'_{min}) =$$

$$\frac{2/\lambda}{\sqrt{3(4-4x+3x^2)}}\{(2-3x)\cos\theta'_{min} + \sqrt{8}\sin\theta_{min}\} \quad (B8)$$

$$= \sqrt{4-4x+3x^2}\,a^* \quad (B9)$$

$$(4-4x+3x^2)\frac{a^*\lambda}{2}\sqrt{3} = (2-3x)\cos\theta'_{min} + \sqrt{8}\sin\theta'_{min} \quad (B10)$$

From (B5) and (B10),

$$\frac{4-4x+3x^2}{3+2x+3x^2} = \frac{(2-3x)\cos\theta'_{min} + \sqrt{8}\sin\theta'_{min}}{(1+3x)\cos\theta_{min} + \sqrt{8}\sin\theta_{min}} \quad (B11)$$

Since θ_{min} and θ'_{min} can be measured from experimental data, it is possible to determine x from equation (B11).

REFERENCES

1 Hachisu, S., Kobayashi, Y. and Kose, A. *J. Colloid. Interface Sci.* 1973, **42**, 342
2 Ise, N., Okubo, T., Sugiura, M., Ito, K. and Nolte, H. J. *J. Chem. Phys.* 1983, **78**, 536
3 Sogami, I. *Phys. Letters* 1983, **96A**, 199
4 Hiltner, P. A. and Krieger, I. M. *J. Phys. Chem.* 1969, **73**, 2386
5 Williams, R. and Crandoll, R. S. *Phys. Letters* 1974, **A48**, 225
6 Clark, N. A., Hurd, A. and Ackerson, B. J. *Nature* 1979, **281**, 57; Ackerson, B. J. and Clark, B. J. *Phys. Rev. Letters* 1981, **46**, 123
7 Pieranski, P., Bubois-Violette, E., Rothen, F. and Strzelecki, L. *J. Phys. (Paris)* 1981, **42**, 53; Pieranski, P. *Contemp. Phys.* 1983, **24**, 25
8 Yoshiyama, T., Sogami, I. and Ise, N. *Phys. Rev. Letters* 1984, **53**, 2153
9 James, R. W. 'The Optical Principles of the Diffraction of X-rays', Bell, London, 1967, p. 448
10 Warren, B. E. *Phys. Rev.* 1941, **59**, 693
11 Franklin, R. E. *Acta Cryst.* 1950, **3**, 107
12 Wilson, A. J. C. *Proc. Roy. Soc. Lond.* 1942, **A180**, 277
13 Paterson, M. S. *J. Appl. Phys.* 1952, **23**, 805
14 Kakinoki, J. and Komura, Y. *J. Phys. Soc. Jpn.* 1955, **9**, 169